

## CVFEM coupled with FLO Scheme for Solution to Heat and Fluid Problems

Open  
Access

Mostefa Kaouari<sup>1,\*</sup>, Fodil Hammadi<sup>2</sup>, Belkacem Draoui<sup>3</sup>

<sup>1</sup> Laboratory of Mechanics: Simulation & Experimentation (L2ME), Algeria

<sup>2</sup> TAHRI Mohamed University of Bechar, Algeria

<sup>3</sup> ENERGARID Laboratory, TAHRI Mohamed University of Bechar, Algeria

### ARTICLE INFO

### ABSTRACT

#### Article history:

Received 11 September 2018

Received in revised form 3 February 2019

Accepted 12 May 2019

Available online 15 July 2019

Nowadays, CVFEM has proved to be an effective method for solving real problems in CFD. Combining advantages of CVFDMs with those of FEMs results in an improved method, able to deal with complex geometries, and satisfy local and global conservation principles. To solve dynamical field, a good scheme is always required for discretization of the convective terms. The FLO scheme is opted for in this study, because it is extracted as exact solution from a modified equation. The resolution procedure used is the SIVA. Coding this procedure is achieved using advanced instructions in Fortran 90/95. The presented results, prove a best agreement with benchmarks.

#### Keywords:

CVFE; FLO scheme; SIVA; Fortran 90/95

Copyright © 2019 PENERBIT AKADEMIA BARU - All rights reserved

## 1. Introduction

Control Volume Finite Element Method (CVFEM) is increasingly used in solving fluid flow and heat transfer problems of different complexities. The success reached in merging the two ancient methods in CFD problems (i.e. CVFDM and FEM), increased the field of application CVFEM method. The physical domain is discretized in three nodes triangular elements; every element is subsequently divided in three sub-volumes; this geometrical treatment is achieved by collecting all sub-volumes surrounding the considered node to construct the control volume. In addition, other geometrical information is required in the phase of discretization of conservation and continuity equations. Convective terms present in the momentum equations are very difficult to handle it without specific considerations. These convective terms are approximated by interpolation function that responds to an element Peclet number and take into account the direction of the element average velocity vector. The diffusive terms are interpolated linearly, and there is no reason to use the same scheme used for convective ones. The first eminent work that presents the FLO scheme is Baliga and Patankar [1, 2], the ideas behind this scheme was proposed in the work of Raithby [3-5].

\* Corresponding author.

Email address: [Kaouari\\_must@yahoo.fr](mailto:Kaouari_must@yahoo.fr) (Mostefa Kaouari)

The vast majority of works in the literature propose computing velocities of components and pressure in different places in the grid, using staggered in structured grid, using unequal order or computing pressure at element centroid in the case of unstructured grid. This difficulty was demystified by the work of Rhie and Chow [5], and its adaptation for unstructured grid was proposed by Prakash and Patankar [6]. Equal-order method allows using one single mesh and the discretization satisfies the mass conservation.

## 2. Methodology

### 2.1 Governing Equations

This work is limited to steady flows of incompressible Newtonian fluids. The governing equations of continuity or momentum are given by non-linear partial differential equations expressed in Cartesian coordinates system (x, y).

#### Continuity Equation

$$\frac{\partial(\rho u_i)}{\partial x_i} = 0 \quad (1)$$

#### Momentum Equations

$$\frac{\partial(\rho u_i)}{\partial t} + \frac{\partial(\rho u_i u_j)}{\partial x_j} = -\frac{\partial P}{\partial x_i} + \frac{\partial}{\partial x_j} \left( \mu \frac{\partial u_i}{\partial x_j} \right) + S_{u_i} \quad (2)$$

#### Transport Equation for another scalar variable

$$\frac{\partial(\rho \phi)}{\partial t} + \frac{\partial(\rho u_i \phi)}{\partial x_i} = \frac{\partial}{\partial x_i} \left( \Gamma_\phi \frac{\partial \phi}{\partial x_i} \right) + S_\phi \quad (3)$$

### 2.2 Numerical Method

The CVFEM used in the discretization process of the aforementioned equations, allows converting these equations in system of algebraic equations by integration on control volume surrounding the considered node of the calculation domain (Figure 1).

#### 2.2.1 Transport equation of $\phi$ (general form)

Considering a node from a calculating domain, and by applying all the principles of integration inherent to the method in terms of momentum and continuity equations, all contributions are aggregated in an element-by-element basis, while including terms related to boundary contributions if they exist.

$$\int_{iaoc} \frac{\partial}{\partial t} (\rho \phi) dV + \int_a \bar{J} \cdot \bar{n} ds + \int_o \bar{J} \cdot \bar{n} ds - \int_{iaoc} S_\phi dV \quad (4)$$

The flux  $\bar{J}$  is a combination of two existing fluxes in the principal equation, the diffusion flux  $\bar{J}_D$  and the convection flux  $\bar{J}_C$ .  $\bar{n}$  is normal vector to the surface (one among three),  $ds$  designate its length, Figure 2(a).

$$\bar{J} = \bar{J}_D + \bar{J}_C \tag{5}$$

$$\bar{J}_D = -\Gamma_\phi \nabla \phi \tag{6}$$

$$\bar{J}_C = \rho \bar{V} \phi \tag{7}$$

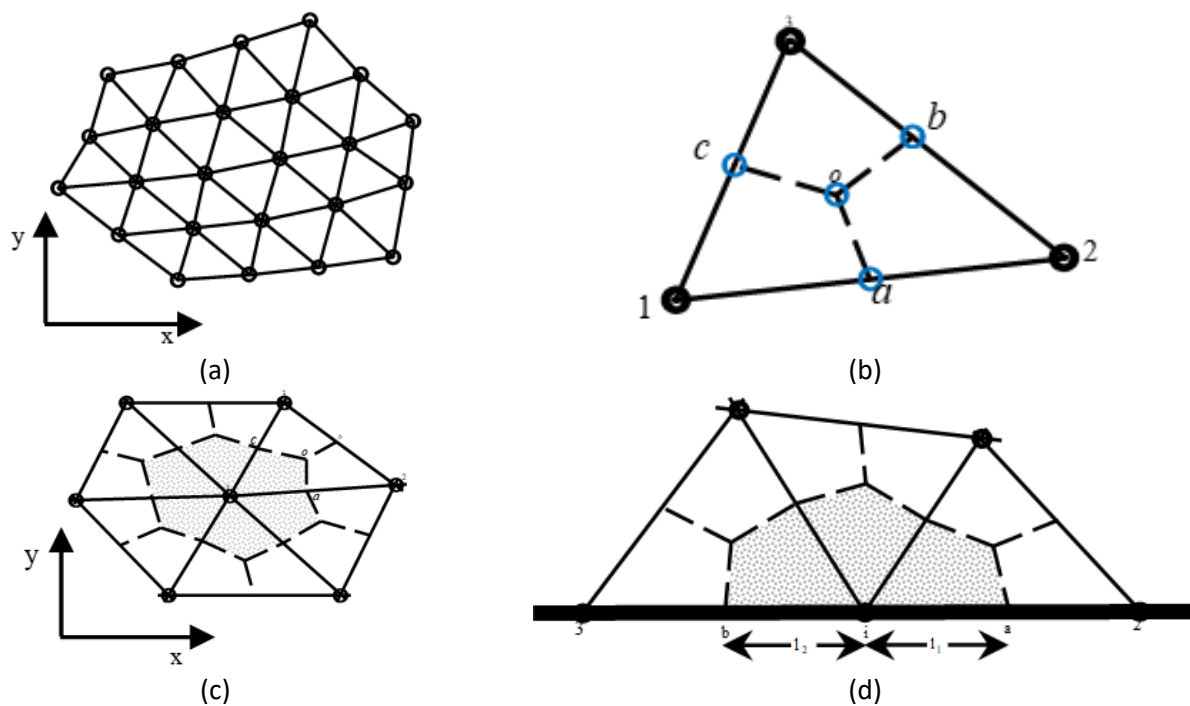


**Fig. 1.** Discretization of calculation domain and nomenclatures: (a) simple domain decomposed on triangular elements; (b) triangular element and its calculated necessary positions; (c) a cell designated by an internal node 1 and all its surrounding elements, control volume associate with it; (d) elements and control volume associated at node i on the boundary

The source term  $S_\phi$  is always expressed under the linear form,  $S_p$  and  $S_c$  are computed at nodes of the calculated domain and their values are assumed to prevail on the portion of the volume belonging to the considered node.

$$S_\phi = S_p \phi + S_c \tag{8}$$

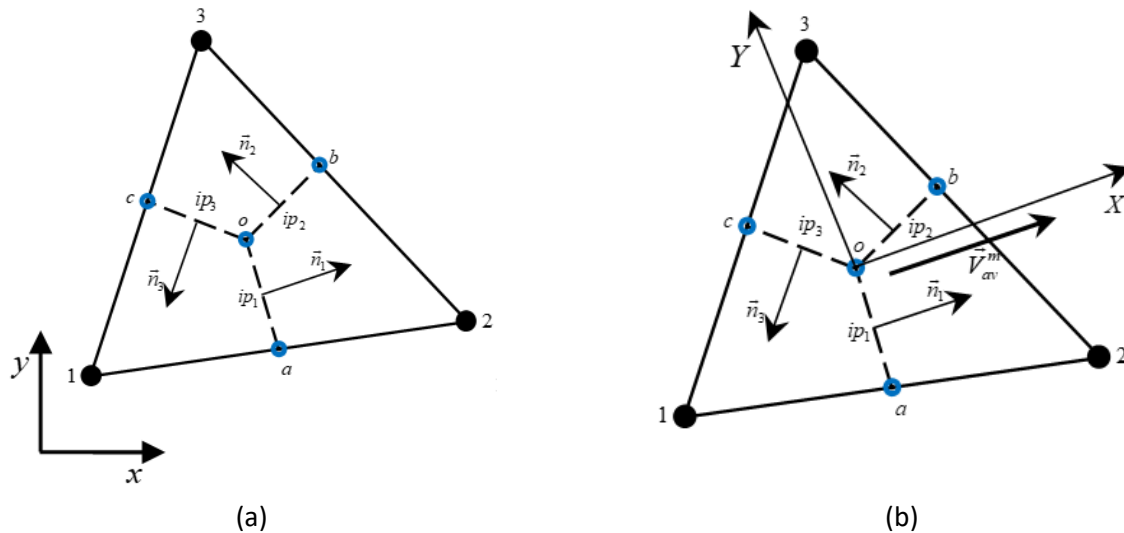


**Fig. 2.** (a) Designation of integration point's  $ip_i$  on the faces a three associated unity vectors  $\bar{n}_i$  on the global coordinate system; (b) visualization of local axes system on the element centroid, X axe is parallel to  $\bar{V}_{av}^m$

## 2.2.2 Interpolation Functions

### 2.2.1.1 Diffusion term

In each element, the dependent variable  $\varphi$  in diffusion term is interpolated linearly.

$$\varphi = A_{\varphi}^D x + B_{\varphi}^D y + C_{\varphi}^D \quad (9)$$

The values of coefficients  $A_{\varphi}^D$ ,  $B_{\varphi}^D$  and  $C_{\varphi}^D$ , can be uniquely expressed in terms of three nodal values of  $x$ ,  $y$  and  $\varphi$  for each element.

### 2.2.1.2 Convection term

For convection term, the scheme of Saabas and Baliga [2, 7-9], and others are used in this work. Strong convection relative to moderate diffusion transport can happen, linear interpolation of the advection term lead to unrealistic oscillatory solution or divergence of all the iterative solution procedure.

$$\varphi^C = A_{\varphi}^C \xi + B_{\varphi}^C Y + C_{\varphi}^C \quad (10)$$

$$\xi = \frac{\Gamma_{\varphi}}{\rho U_{av}^m} \left[ \exp\left(\frac{P_e (X - X_{max})}{X_{max} - X_{min}}\right) - 1 \right] \quad (11)$$

$$P_e = \frac{\rho U_{av}^m (X_{max} - X_{min})}{\Gamma_{\varphi}} \quad (12)$$

$$\begin{cases} X_{max} = \text{MAX}(X_1, X_2, X_3) \\ X_{min} = \text{MIN}(X_1, X_2, X_3) \end{cases} \quad (13)$$

The new local axes system (X, Y) is oriented parallel to the direction of  $\vec{v}_{av}^m$  Figure 2(b). The variable  $\xi$  present in Eq. (11) express exponential variations in the flow direction. Coefficients  $A_\phi^C$ ,  $B_\phi^C$  and  $C_\phi^C$  are functions of nodal values of  $\phi$ , Y and  $\xi$ .

$$U_{av}^m = |\vec{V}_{av}^m| \quad (14)$$

$$\vec{V}_{av}^m = u_{av}^m \vec{i} + v_{av}^m \vec{j} \quad (15)$$

$$u_{av}^m = \frac{u_1^m + u_2^m + u_3^m}{3}; v_{av}^m = \frac{v_1^m + v_2^m + v_3^m}{3} \quad (16)$$

### 2.2.1.3 Equation discretization

Now all necessary components are present to apply the integration on the three faces insight the element. However, it should be noted at diffusion terms are integrated directly, but advection terms are integrated by Simpson mean of 1/3 rule. The final algebraic expression for node i is obtained by assembling procedure for all element's contributions sharing the same node.

$$a_i^\phi \phi_i = \sum_{nb} a_{nb}^\phi \phi_{nb} + b_i^\phi \quad (17)$$

$$a_i^\phi = \sum_{nb,i} a_{nb,i}^\phi - \sum_{\substack{elem.assoc.with \\ elem}} (S_{P,i}^\phi) \quad (18)$$

$$b_i^\phi = \sum_{elem.assoc.with i} (S_{C,i}^\phi \cdot V_{elem} / 3) \quad (19)$$

### 2.2.1.4 Momentum equations discretization

From the additional existence terms of pressure gradients in momentum equations, a close similarity exists between momentum equations and general form equation of transported scalar  $\phi$ . Therefore, for an optimized programming routine, it's advantageous and rational to implement only one general procedure, while adding adequate terms if necessary, such as in Eq. (20). Finally, an assembling procedure is conceived for obtaining algebraic equations in compact form Eq. (21).

$$\int_{iaoc} \left( -\frac{\partial p}{\partial x_j} \right) dV = - \left( \frac{\partial p}{\partial x_j} \right)_{elem} V_{iaoc} \quad (20)$$

$$a_i^{u_j} (u_j)_i = \sum_{nb} a_{nb}^{u_j} (u_j)_{nb} + b_i^{u_j} - \left( \overline{\frac{\partial p}{\partial x_j}} \right) \cdot V_i \quad (21)$$

Additional terms  $\overline{(\partial P / \partial x_j)} \cdot V_i$  represent volume averaged pressure-gradients associated with the control volume surrounding node  $i$ .

$$(\mathbf{u}_j)_i = (\hat{\mathbf{u}}_j)_i - d_i^{u_j} \left( \overline{\frac{\partial p}{\partial x_j}} \right) \quad (22)$$

$$(\hat{\mathbf{u}}_j)_i = \frac{\sum_{nb} a_{nb}^{u_j} (\mathbf{u}_j)_{nb} + b_i^{u_j}}{a_i^{u_j}} \quad (23)$$

$$d_i^{u_j} = \frac{V_i}{a_i^{u_j}} \quad (24)$$

The interpolation functions used to approximate components of velocities in the mass-flux terms are defined as

$$u_i^{m_j} = \hat{u}_i^j - d_o^{u_j} \left( \frac{\partial p}{\partial x_i^j} \right)_{elem} \quad (25)$$

### 2.2.1.5 Depression equation

The mass conservation equation for a control-volume surrounding node  $i$  can be written as

$$\int_a^o \rho \bar{V}^m \cdot \bar{n} ds + \int_o^c \rho \bar{V}^m \cdot \bar{n} ds \quad (26)$$

However, it's important to note that the pressure must be expressed by its interpolation function which have a linear form, pressure gradients are exactly the coefficients of the pressure interpolation function.

$$p = A^P x + B^P y + C^P \quad (27)$$

Similar to the  $\phi$  coefficients, here too, interpolation function coefficients are themselves functions of considered element nodal pressure.

After integration on faces insight the element after developing a suitable assembling procedure of all other elements surrounding node  $i$ , the algebraic equations are obtained and written in its compact form as

$$a_i^p p_i = \sum_{nb} a_{nb}^p p_{nb} + b_i^p \quad (28)$$

where,

$$a_i^p = \sum_{nb} a_{nb}^p \quad (29)$$

### 2.2.1.6 Boundary conditions

To obtain final algebraic equations by grouping all above mentioned contributions, boundary conditions must be included properly.

If the value of dependent variable is specified on a portion of the boundary, then the suitable treatment is as

$$a_i^\phi = 1, a_{nb}^\phi = 0, b_i^\phi = \phi_{spec} \quad (30)$$

If the known transported scalar is a component of velocity, additional operation is carried out, the coefficient of pressure gradient becomes null and pseudo-velocity obtain the velocity value.

For specified flux condition, the total flux of  $\phi$  normal to the boundary is given by the expression

$$\vec{J} \cdot \vec{n} = \rho V_n \phi - \Gamma_\phi \left( \frac{\partial \phi}{\partial n} \right)_{spec} \quad (31)$$

If outflow condition is considered, the diffusion term is negligible compared to the convection term, for this reason the term  $\Gamma_\phi \left( \frac{\partial \phi}{\partial n} \right)$  is eliminated from equation.

### 2.2.1.7 Under-relaxation

Following the proposition of Patankar [10], under-relaxation is a very useful to handle the strong non-linearity found in discretized equations of Navier-Stokes equations, dependent variables values change hugely from iteration to the successive one. The E-factor method is retained in the code developed in the context of this work. The values of E proposed are 1 for the components of velocity and pressure, and 5 for temperature.

$$a_i^{u_j} \left( 1 + \frac{1}{E^i} \right) (u_j)_i = \sum_{nb} a_{nb}^{u_j} (u_j)_{nb} + a_j^p P_j + \sum_{nb} a_{nb}^p P_{nb} + b_i^{u_j} + \frac{a_i^{u_j}}{E^i} (u_j)_i \quad (32)$$

## 2.3 Resolution Algorithm

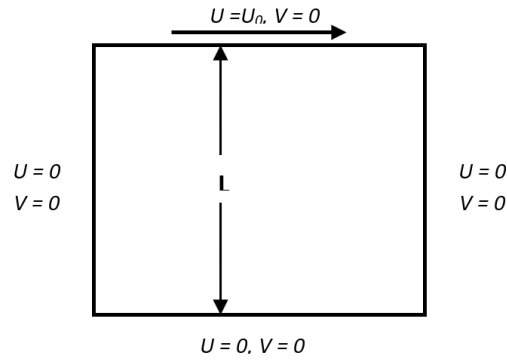
The acronym SIVA “Sequential Iterative Variable Adjustment” is the solution procedure adopted in this work thanks to its very simple implementation. The reader is invited to survey the relevant works in literature, to have a firm grasp of steps followed in this algorithm.

## 3 Results

### 3.1 Validation Tests

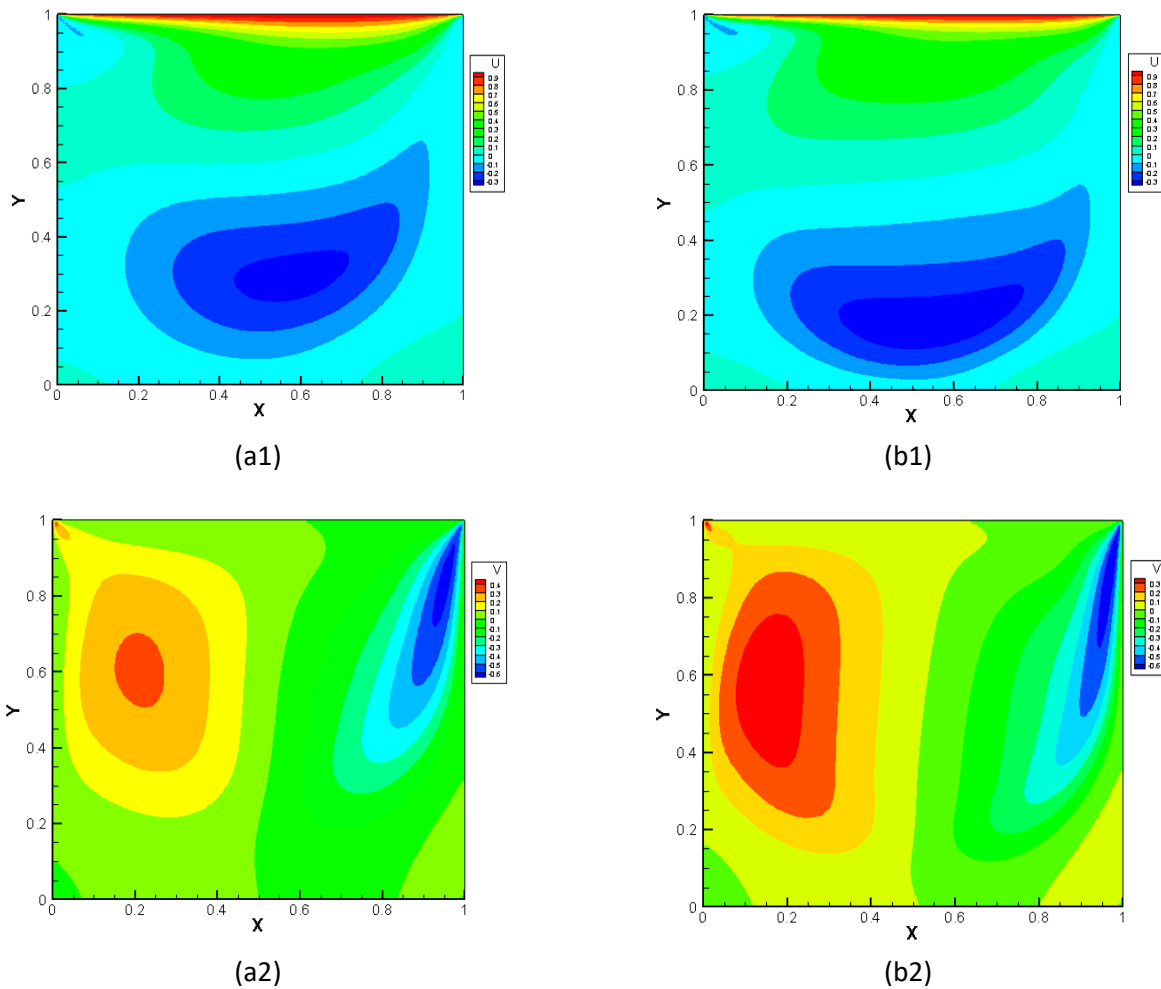
#### 3.1.1 Lid driven cavity

This benchmark is an important two-dimensional laminar incompressible fluid flow. The fluid is moved by a horizontal velocity on the upper wall, while the other three are subject to the adhesion condition. This problem depends on the values of Reynolds number which can give dominance to the convection terms when its value is high enough. In addition, there are two singularity located on the bottom corners of the cavity, locations where arise secondary recirculation cells in addition to the primary cell that dominate the majority of the space of the cavity. The geometry of the problem is as shown in Figure 3.



**Fig. 3.** Lid driven cavity Geometry and boundary conditions

The results obtained are compared with Ghia *et al.*, [11] and Tran *et al.*, [12] (as shown in Figure 4). A comparative table is drawn below (Table 1) to show the superiority this work against results given by works of Tran *et al.*, [12].



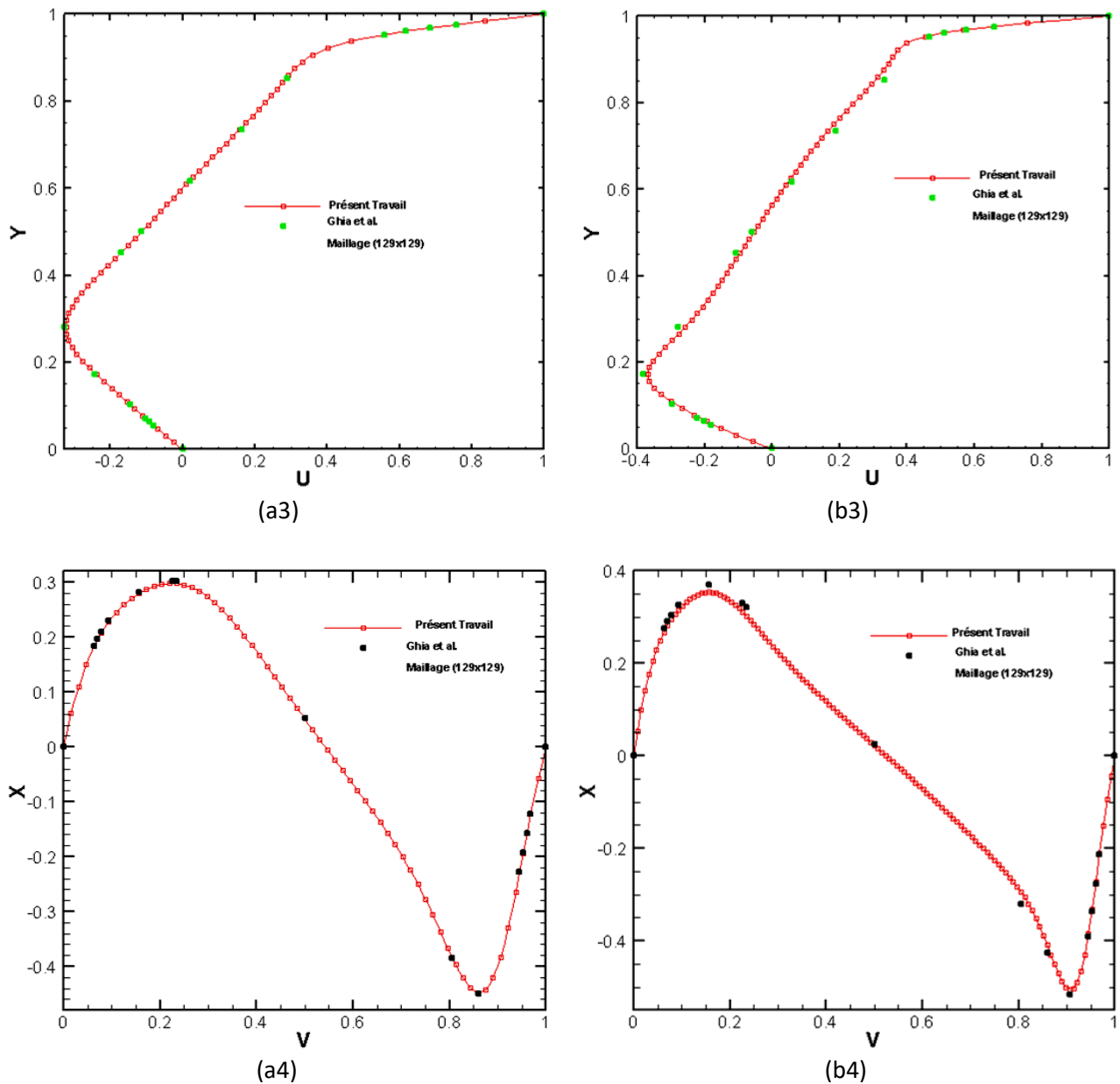


**Fig. 4.** Visualization of velocity components  $u$  and  $v$  (a1), (a2) for  $Re = 400$ ; (b1) and (b2) for  $Re = 10^3$ . Visualization of velocity profiles for  $u$  at  $x=0.5$  and  $v$  at  $y=0.5$  are given in (a3), (a4) for  $Re = 400$  and in (b3) and (b4) for  $Re = 10^3$

**Table 1**  
 Comparison of Results,  $Re = 400$

	Grid	$U_{min}$	$V_{max}$	$V_{min}$
Tran <i>et al.</i> ,	32x32	-.25841	.24042	-.37622
Present work		-.28096	.25876	-.39411
Tran <i>et al.</i> ,	64x64	-.30192	.27823	-.42476
Present work		-.30903	.28525	-.43168
Tran <i>et al.</i> ,	129x129	-.32052	.29548	-.44475
Present work		-.32286	.29824	-.44743
Ghia <i>et al.</i> ,	129x129	-.3273	.3020	-.4499

### 3.1.2 Natural convection

A square cavity side  $L$  containing fluid in motion caused by a difference in temperature between the two sides right and left one. The two other sides are adiabatic, see Figure 5. This difference in temperature levels excites the fluid to circulate into the cavity (as shown in Figure 6). The Boussinesq hypothesis is valuable here. The Prandtl number has the value 0.72 and the Rayleigh number varies between  $10^3$  and  $10^6$ . Here too, the code built in this work proves its superiority, its results are very close to those of De Vahl Davis [13] than those given by the works of Wan *et al.*, [14] and Veronique Feldheim [15]. Table 2 and Table 3 confirm these findings.

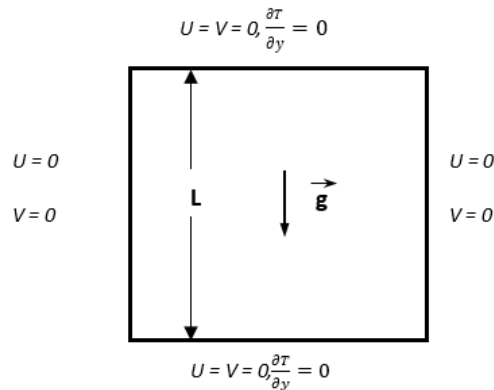


**Fig. 5.** Cavity of natural convection and boundary conditions

**Table 2**

Comparison of results,  $Ra = 10^3$  and  $10^4$

$Ra = 10^3$	$U_{max}$	$V_{max}$	$Ra = 10^4$	$U_{max}$	$V_{max}$
De Vahl Davis, 1983	3.649	3.697		16.178	19.617
Wan <i>et al.</i> , 2001 (DSC)	3.643	3.686		15.967	19.98
Wan <i>et al.</i> , 2001 (FEM)	3.489	3.686		16.122	19.79
Veronique Feldheim					
41x41	3.629	3.674	41x41	16.025	19.610
81x81	3.644	3.689	81x81	16.077	19.703
161x161	3.649	3.692	161x161	16.098	19.730
Present Work					
33x33	3.6418	3.6842	33x33	16.056	19.5724
81x81	3.6483	3.6954	81x81	16.1643	19.5999
161x161	3.6492	3.6964	161x161	16.1746	19.6348

**Table 3**

Comparison of results,  $Ra = 10^5$  and  $10^6$

$Ra = 10^5$	$U_{max}$	$V_{max}$	$Ra = 10^6$	$U_{max}$	$V_{max}$
De Vahl Davis, 1983	34.73	68.59		64.63	219.36
Wan <i>et al.</i> , 2001 (DSC)	33.51	70.81		65.55	227.24
Wan <i>et al.</i> , 2001 (FEM)	33.39	70.63		65.40	227.11
Veronique Feldheim					
41x41	33.73	70.09	41x41	65.19	225.06
81x81	33.52	70.251	81x81	65.397	226.60
161x161	33.443	70.549	161x161	65.418	226.62
Present Work					
33x33	33.936	68.679	33x33	60.1161	215.666
81x81	34.544	68.613	81x81	63.7264	220.660
161x161	34.633	68.654	161x161	64.4546	220.786

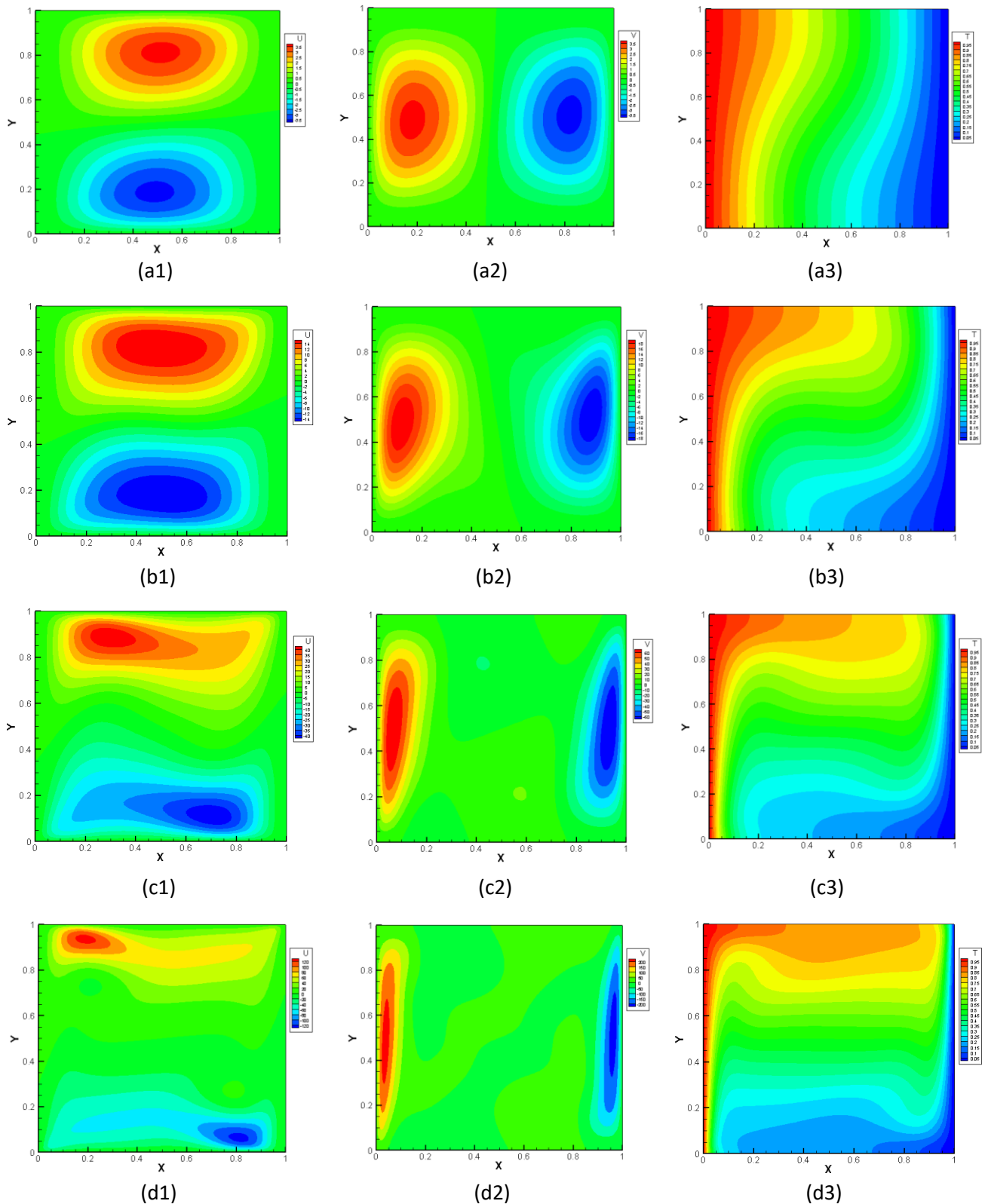


**Fig. 6.** The field of velocity components  $u$ ,  $v$  and temperature fields are displayed according to the value of the Rayleigh number. For  $Ra = 10^3$  the results are in Figure (a1), (a2) and (a3). For  $Ra = 10^4$  the results are in Figure (b1), (b2) and (b3). For  $Ra = 10^5$  the results are in Figure (c1), (c2) and (c3). For  $Ra = 10^6$  the results are in Figure (d1), (d2) and (d3)

#### 4. Conclusions

During the elaboration of this work, the aim was Saabas reproduction work [2, 7-9] mentioned in many references; the idea is to see the impact of advanced object-oriented programming with Fortran 90/95 language on the results quality.

Despite recent criticisms made in the work of Lamoueux *et al.*, [16], the obtained results show superiority compared to those found in the literature. Moreover, the algorithm implementation is simple and straightforward, and no need for necessary a velocity components correction or pressure. The only existent inconvenient in this solution procedure is the zero-value affectation to the pressure gradients coefficients at the boundary where the velocity components are known.

#### References

- [1] Baliga, B. R. "A Control-Volume Based Finite Element Method for Convective Heat and Mass Transfer." Ph.D. Thesis, University of Minnesota, Minneapolis, U.S.A., 1978.
- [2] Baliga, B. R., and S. V. Patankar. "A new finite-element formulation for convection-diffusion problems." *Numerical Heat Transfer* 3, no. 4 (1980): 393-409.
- [3] Raithby, G. D. "A critical evaluation of upstream differencing applied to problems involving fluid flow." *Computer Methods in Applied Mechanics and Engineering* 9, no. 1 (1976): 75-103.
- [4] Raithby, G. D. "Skew upstream differencing schemes for problems involving fluid flow." *Computer Methods in applied mechanics and engineering* 9, no. 2 (1976): 153-164.
- [5] Rhie, C. M., and W. Li Chow. "Numerical study of the turbulent flow past an airfoil with trailing edge separation." *AIAA journal* 21, no. 11 (1983): 1525-1532.
- [6] Prakash, Ch, and S. V. Patankar. "A control volume-based finite-element method for solving the Navier-Stokes equations using equal-order velocity-pressure interpolation." *Numerical Heat Transfer* 8, no. 3 (1985): 259-280.
- [7] Saabas, H. J. "A control volume finite element method for three-dimensional, incompressible, viscous fluid flow. Dept. of." *Mech. Eng., McGill University, Montreal, Que, Canada. Ph. D. Thesis* (1991).
- [8] Saabas, H. J., and B. R. Baliga. "CO-LOCATED EQUAL-ORDER CONTROL-VOLUME FINITE-ELEMENT METHOD FOR MULTIDIMENSIONAL, INCOMPRESSIBLE. FLUID FLOW-PART I: FORMULATION." *Numerical Heat Transfer* 26, no. 4 (1994): 381-407.
- [9] Saabas, H. J., and B. R. Baliga. "Co-located equal-order control-volume finite-element method for multidimensional, incompressible, fluid flow—Part II: verification." *Numerical Heat Transfer* 26, no. 4 (1994): 409-424.
- [10] Baliga, B. R., and S. V. Patankar. "A new finite-element formulation for convection-diffusion problems." *Numerical Heat Transfer* 3, no. 4 (1980): 393-409.
- [11] Ghia, U. K. N. G., Kirti N. Ghia, and C. T. Shin. "High-Re solutions for incompressible flow using the Navier-Stokes equations and a multigrid method." *Journal of computational physics* 48, no. 3 (1982): 387-411.
- [12] Dung Tran, Luu, Christian Masson, and Arezki Smaïli. "A stable second-order mass-weighted upwind scheme for unstructured meshes." *International Journal for numerical methods in fluids* 51, no. 7 (2006): 749-771.
- [13] de Vahl Davis, G. "Natural convection of air in a square cavity: a bench mark numerical solution." *International Journal for numerical methods in fluids* 3, no. 3 (1983): 249-264.
- [14] C. Wan, BSV Patnaik, GW Wei, D. "A new benchmark quality solution for the buoyancy-driven cavity by discrete singular convolution." *Numerical Heat Transfer: Part B: Fundamentals* 40, no. 3 (2001): 199-228.
- [15] Véronique Feldheim, Simulation Numérique des Transferts Thermiques Combinés Conduction, Convection, Rayonnement dans des Domaines de Géométrie Complexe, Docteur en Sciences Appliquées, Faculté Polytechnique de Mons, 2002.
- [16] Lamoueux, Alexandre, and B. Rabi Baliga. "Improved formulations of the discretized pressure equation and boundary treatments in co-located equal-order control-volume finite-element methods for incompressible fluid flow." *Numerical Heat Transfer, Part B: Fundamentals* 59, no. 6 (2011): 442-472.